ELSEVIER

Thermochimica Acta 381 (2002) 153–164

thermochimica
acta

www.elsevier.com/locate/tca

# Thermal characterization and physicochemical properties of $Fe_2O_3$–$Mn_2O_3/Al_2O_3$ system

W.M. Shaheen[a,*], K.S. Hong[b]

[a]*Laboratory of Surface Chemistry and Physical Chemistry, Physical Chemistry Department,*
*National Research Center, El-Tahrir St., Dokki, Cairo, Egypt*
[b]*Physics Department, Korean Basic Science Institute, Seoul 136-701, South Korea*

Received 20 February 2001; accepted 13 June 2001

## Abstract

The effect of ferric and manganese oxide dopants on thermal and physicochemical properties of Mn-oxides/$Al_2O_3$ and $Fe_2O_3/Al_2O_3$ systems has been studied separately. The pure and doped mixed solids were prepared by impregnation method, then thermally treated at (400–1000 °C). Pyrolysis of pure and doped mixed solids was investigated via thermal analysis (thermogravimetry (TG) and differential thermogravimetry (DTG)) techniques. The thermal products were characterized by means of X-ray diffraction (XRD) analysis. The catalytic behavior of the thermal products was tested using the decomposition of $H_2O_2$ reaction. The results revealed that pure ferric nitrate decomposes into $Fe_2O_3$ at 350 °C and shows thermal stability up to 1000 °C. Pure manganese nitrate yields $MnO_2$ at 300 °C and $Mn_2O_3$ at 500 °C and $Mn_3O_4$ at 1000 °C. Crystalline $\gamma$-$Al_2O_3$ phase was detected for all samples preheated up to 800 °C. Ferric and manganese oxides enhanced the crystallization of $\alpha$-$Al_2O_3$ phase at 1000 °C. Each of ferric, manganese, and aluminum oxides have thermal effect on the thermal decomposition products of the mixed components. Crystalline $MnAl_2O_4$ and $MnFe_2O_4$ phases were formed at 1000 °C as a result of solid–solid interactions between the corresponding thermal products. $Fe_2O_3$ doping increased the catalytic activity of $Mn_2O_3/Al_2O_3$ system up to certain limit, and has an inhibiting effect by increasing its content above this limit. The catalytic activity of $Fe_2O_3/Al_2O_3$ system progressively increased with increasing the manganese oxide dopant.

*Keywords:* Thermal decomposition; Doping; Characterization; Solid–solid interaction

## 1. Introduction

The thermal decomposition and the physicochemical properties of the loaded solid are dependent, mainly on many factors such as preparation method [1], the calcination conditions [2], doping with certain foreign cations [3,4] and also on the extent of loading [5]. Alumina is the most convenient support for the catalysts employed in the oxidation reduction reactions [6,7]. This is because of its high surface area, and porous structure [8]. Also, alumina greatly increases the degree of dispersion of the catalytically active constituents, hindering their grain growth and thus increasing the activity and durability of the supported catalyst [9]. On the other hand, the combination of transition metal oxides may result in modifications in their thermal behavior, geometric structures, and electronic properties that lead to changes in their catalytic functions [10]. The present work is devoted to a study of the thermal and physicochemical properties of manganese nitrate supported

---

[*] Corresponding author. Fax: +20-2-3370931.
*E-mail address*: shaheen40@hotmail.com (W.M. Shaheen).

PII: S0040-6031(01)00652-9

on aluminum hydroxide system and ferric nitrate supported on aluminum hydroxide system fired at different reaction temperatures in the pure state and influenced by doping with different portions of ferric and manganese oxides separately. The techniques employed were thermal analysis (thermogravimetry (TG) and differential thermogravimetry (DTG)) and the X-ray diffraction (XRD) analysis. The catalytic activities of the pure and doped mixed solids were tested in hydrogen peroxide decomposition of reaction at 30, 40, and 50 °C.

## 2. Experimental

### 2.1. Materials

The starting materials used in this investigation were ferric nitrate hydrated, $Fe(NO_3)_3 \cdot 9H_2O$, and manganese nitrate tetrahydrate, $Mn(NO_3)_2 \cdot 4H_2O$. These chemicals were provided by Fluka Company. Aluminum hydroxide, $Al(OH)_3$, solid provided by Prolabo Company. The specific surface area $S_{BET}$ of the employed $Al(OH)_3$ precalcined in air at 500 °C for 4 h was determined from the $N_2$ adsorption isotherm at $-196$ °C and was found to be 235 $m^2\,g^{-1}$.

### 2.2. Method of preparation of pure and doped solids

A known mass of finely powdered $Al(OH)_3$ was impregnated with a solutions containing definite amount of manganese nitrate tetrahydrate, expressed in mol% of $Mn_2O_3$, and fixed at 20. The obtained pastes were dried at 100 °C. A series of dried pastes were doped with different portions of ferric nitrate solutions and then dried again at 100 °C. The obtained solids were calcined in air at 400–1000 °C for 4 h in air atmosphere. On the other hand, following the same procedure series of pure mixture of ferric nitrate, expressed in mol% of $Fe_2O_3$, and fixed at 20, supported on aluminum hydroxide and mixtures of it doped with different portions of manganese nitrate and calcined at the same temperature. The dopant concentration of both ferric and manganese nitrate were calculated with respect to $Fe_2O_3$ and $Mn_2O_3$ and fixed to be 1.96, 3.85, 7.41, and 16.67 mol% for each other. Table 1 shows the symbols and the composition of the pure and doped mixtures, which were thermally treated at reaction temperatures of 400, 600, 800, and 1000 °C.

Table 1
Symbols and composition of the pure and doped mixtures[a]

| Symbol | Composition |
|---|---|
| Mn–Al (I) | 0.50 $Mn(NO_3)_2 \cdot 4H_2O$/2.0 $Al(OH)_3$ |
| Fe–Mn–Al (II) | 0.05 $Fe(NO_3)_3$–0.5 $Mn(NO_3)_2$/2.0 $Al(OH)_3$ |
| Fe–Mn–Al (III) | 0.10 $Fe(NO_3)_3$–0.5 $Mn(NO_3)_2$/2.0 $Al(OH)_3$ |
| Fe–Mn–Al (IV) | 0.20 $Fe(NO_3)_3$–0.5 $Mn(NO_3)_2$/2.0 $Al(OH)_3$ |
| Fe–Mn–Al (V) | 0.50 $Fe(NO_3)_3$–0.5 $Mn(NO_3)_2$/2.0 $Al(OH)_3$ |
| Fe–Al (VI) | 0.50 $Fe(NO_3)_3 \cdot 9H_2O$/2.0 $Al(OH)_3$ |
| Mn–Fe–Al (VII) | 0.05 $Mn(NO_3)_2$–0.5 $Fe(NO_3)_3$/2.0 $Al(OH)_3$ |
| Mn–Fe–Al (VIII) | 0.10 $Mn(NO_3)_2$–0.5 $Fe(NO_3)_3$/2.0 $Al(OH)_3$ |
| Mn–Fe–Al (IX) | 0.20 $Mn(NO_3)_2$–0.5 $Fe(NO_3)_3$/2.0 Al(OH)3 |
| Mn–Fe–Al (X) | 0.50 $Mn(NO_3)_2$–0.5 $Fe(NO_3)_3$/2.0 $Al(OH)_3$ |

[a] Thermally treated at reaction temperatures of 400, 600, 800, and 1000 °C.

### 2.3. Physical measurements

TG–DTG were carried out on a Shimadzu DT-40 thermal analyzer. The sample was placed in a platinum crucible (0.1 $cm^3$). The samples were studied under air atmosphere with flowing rate of 30 ml $min^{-1}$. The size of samples were selected to be about 7–16 mg. $\alpha$-$Al_2O_3$ was used as a reference in this technique. The rate of heating was 10 °C $min^{-1}$.

XRD patterns were obtained at room temperature using a Philips X-ray diffractometer (Goniometer PW1050/50), employing copper radiation as the X-ray source. The X-ray tube was operated at 36 kV and 16 mV. Samples were finely ground and packed in a plastic holder. The diffraction angle of $2\theta$ was scanned at a rate of 2° $min^{-1}$.

The catalytic decomposition of hydrogen peroxide was used as a model reaction for determining the catalytic activity of pure and doped mixed solids thermally treated at 400, 600, 800, and 1000 °C and at reaction temperatures 30, 40, and 50 °C. The reaction was followed up through a gasometric measurement of evolved oxygen [10].

## 3. Results and discussion

### 3.1. Thermal analysis and XRD characterization of $Fe(NO_3)_3 \cdot 9H_2O$

Fig. 1a shows the TG–DTG curves of the pure ferric nitrate hydrate. It can be seen that the step starts at

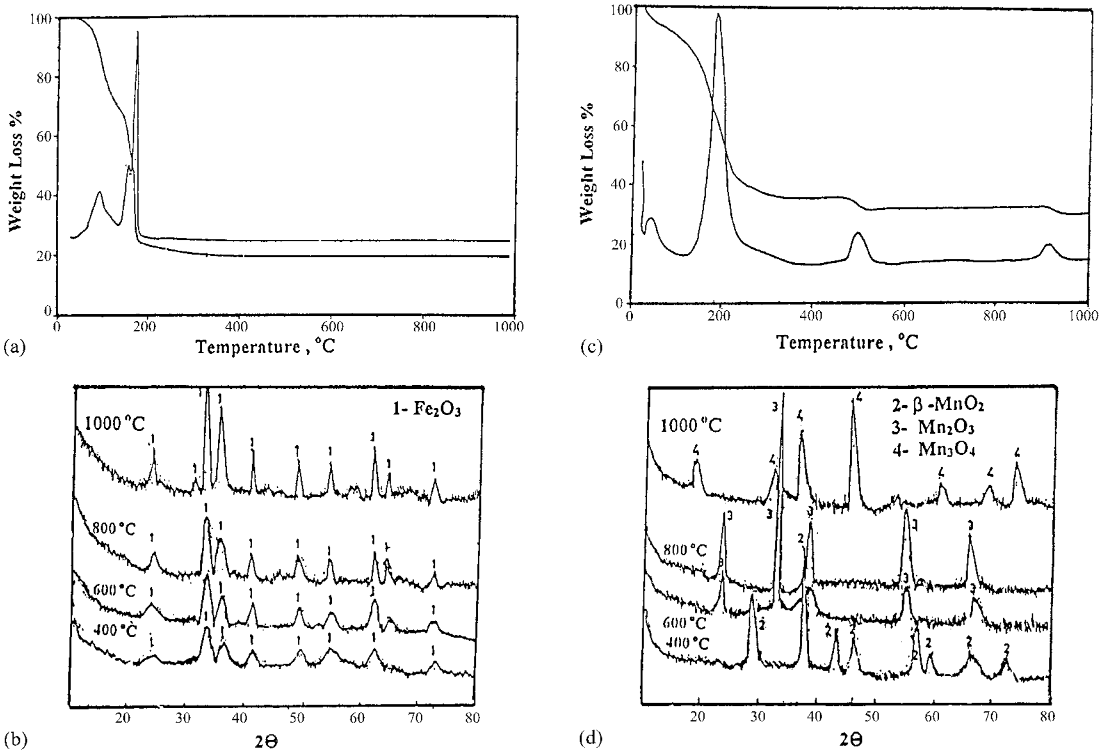

Fig. 1. (a) Thermal analysis (TG–DTG) of pure hydrated ferric nitrate; (b) X-ray diffractogram of ferric nitrate preheated at 400, 600, 800, and 1000 °C; (c) thermal analysis (TG–DTG) of pure hydrated manganese nitrate; (d) X-ray diffractogram of manganese nitrate preheated at 400, 600, 800, and 1000 °C.

about 190 °C with a constant weight loss of 78% correspond to the formation of Fe(OOH) [11]. The last step starts at temperature higher than 350 °C accompanied by a constant weight loss of 80% which might characterize the formation of $Fe_2O_3$ [12] which is thermally stable up to 1000 °C.

On the other hand, Fig. 1b represents the X-ray diffractograms of pure ferric nitrate precalcined at 400–1000 °C. It shows the formation of $\alpha$-$Fe_2O_3$ (rhombohedral) phase [12] at different treatment temperatures. The degree of crystallinity of the formed phase increased with increasing the calcination temperature up to 1000 °C.

### 3.2. Thermal analysis and XRD characterization of $Mn(NO_3)_2{\cdot}4H_2O$

Fig. 1c represents the TG–DTG curves of pure manganese nitrate tetrahydrate. The result showed that the pure salt decomposes into $MnO_2$ [13,14] at about 300 °C with a constant weight loss of 65.5%. Then, converted to $Mn_2O_3$ at about 500 °C with a constant weight loss of 68.5%. The last step starts at about 900 °C, and accompanied by a constant weight loss of 70% due to the formation of $Mn_3O_4$ [10].

On the other hand, the X-ray investigation of pure manganese nitrate, represented on Fig. 1d, showed the formation of poorly crystalline $\beta$-$MnO_2$ (tetragonal) phase [13] at 400 °C. The thermal treatment of the solid at 600 °C yields crystalline $Mn_2O_3$ (cubic) phase; its degree of crystallinity increased with increasing calcination temperature up to 800 °C. At 1000 °C, the X-ray diffractogram conformed the formation of well-crystalline $Mn_3O_4$ (heximanite) phase [15].

### 3.3. Thermal analysis and XRD characterization of mixture Mn–Al (I)

Fig. 2a showed that the TG–DTG curve of the mixture Mn–Al (I) consists of four steps for the

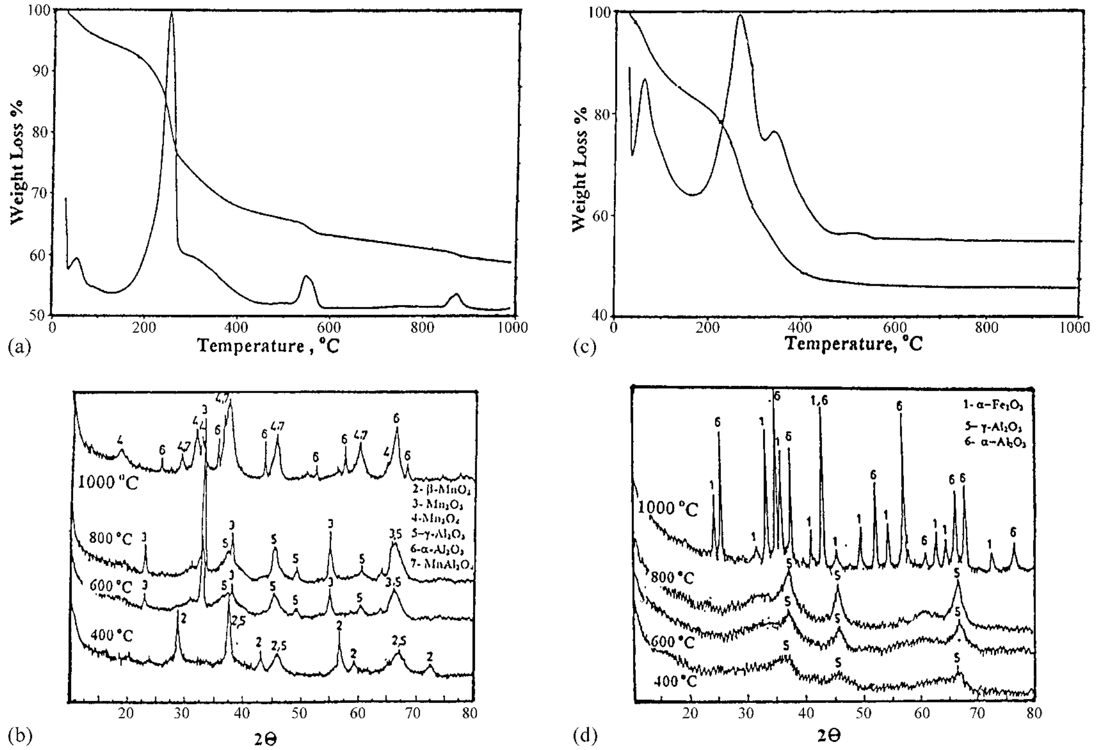

Fig. 2. (a) Thermal analysis (TG–DTG) of mixture Mn–Al (I); (b) X-ray diffractogram of mixture Mn–Al (I) preheated at 400, 600, 800, and 1000 °C; (c) thermal analysis (TG–DTG) of mixture Fe–Al (VI); (d) X-ray diffractogram of Fe–Al (VI) preheated at 400, 600, 800, and 1000 °C.

thermal decomposition process. The first one starts at 80 °C reaching a constant weight loss of 5.5% corresponding to the evolution of all the water. The second step starts at about 200 °C reaching a constant weight loss of 33% at about 425 °C corresponding to the formation of manganese dioxide [13] and aluminum oxyhydroxide compound. The third step starts at about 520 °C with weight loss of 2.8% which is accompanied by the reduction of manganese dioxide to manganese trioxide and also represents complete decomposition of aluminum oxyhydroxide compound to aluminum oxide. The last step starts at about 880 °C reaching a constant total weight loss of 43.5% at about 970 °C. This step might represent the conversion of $Mn_2O_3$ to $Mn_3O_4$ and formation of some portion of $MnAl_2O_4$ as a result of solid–solid interaction between the corresponding oxides, which will be confirmed later by the XRD investigation of this mixture.

On the other hand, X-ray investigation of the mixture Mn–Al (I) preheated at 400, 600, 800, and 1000 °C is illustrated in Fig. 2b, from where it can be seen that poorly crystalline β-$MnO_2$ and γ-$Al_2O_3$ phases are detected at 400 °C. The pretreatment at 600 °C yielded well-crystalline $Mn_2O_3$ (cubic) phase beside poorly crystalline γ-$Al_2O_3$ phase. The degree of crystallinity of both phases increased with increasing the calcination temperature up to 800 °C, and is less than that obtained from treatment of pure manganese nitrate at 400–800 °C. This might be attributed to the presence of aluminum oxide that leads to increase in the degree of dispersion of manganese oxides on its surface, thus hindering their grain growth [16]. On the other hand, further increase of calcination temperature up to 1000 °C yielded a crystalline manganese aluminate phase as a result of solid–solid interaction between the thermal products according to the following equation:

$$Mn_2O_3 + 2Al_2O_3 \rightarrow 2MnAl_2O_4 + \tfrac{1}{2}O_2$$

Also, crystalline $Mn_3O_4$ and α-$Al_2O_3$ were detected. The formation of the latter phase reflects the role of manganese oxide which enhances the ordering process of alumina in the alpha-form [7,17] at this temperature.

### 3.4. Thermal analysis and XRD characterization of mixture Fe–Al (VI)

Fig. 2c showed three steps for thermal decomposition of the mixture Fe–Al (VI) which were accompanied with total weight losses of 15.5 and 53.5%. The first step corresponds to the loss of all water from the mixture and starting the decomposition of aluminum hydroxide to aluminum oxyhydroxide compound at about 215 °C. The second step starts at 405 °C reaching a constant total weight loss of 52% which might correspond to the complete decomposition of aluminum hydroxide to aluminum oxide and the formation of Fe(OOH) compound. The last step starts at about 530 °C with total weight loss of 23.5% corresponding to the complete decomposition of the mixture Fe–Al (VI) to $Fe_2O_3$ and $Al_2O_3$. This means that the presence of aluminum retarded the decomposition of ferric nitrate to ferric oxide. In contrast, the presence of iron enhanced the thermal decomposition of aluminum hydroxide to $Al_2O_3$.

The X-ray investigation of the mixture Fe–Al (VI) preheated at 400, 600, 800, and 1000 °C is shown in Fig. 2d. It can be seen that no patterns of ferric oxide are detected up to 800 °C. On the other hand, crystalline $\gamma$-$Al_2O_3$ phase was detected from 400 up to 800 °C. In this case, alumina plays as support [17] and greatly increases the degree of dispersion, thus hindering the grain growth of the ferric oxide constituents. On the other hand, thermal treatment of the mixture at 1000 °C led to formation of well-crystalline $\alpha$-$Fe_2O_3$ phase. This phase enhanced the crystallization of $Al_2O_3$ in alpha-form at this temperature.

### 3.5. Thermal analysis of pure mixtures of Mn–Al (I) and Fe–Al (IV) influenced by doping with ferric and manganese nitrates

The thermal analysis of the pure mixtures of Mn–Al (I) influenced by doping with ferric oxide, symbolized by Fe–Mn–Al (IV) and Fe–Mn–Al (V), is represented in Fig. 3a and b. On the other hand, the thermal analysis of the pure mixtures of Fe–Al (I) influenced by doping with manganese oxide, symbolized by Mn–Fe–Al (IX) and Mn–Fe–Al (X), is represented in Fig. 3c and d. From these figures, it can be seen that the main difference between them is that the DTG curves of the mixtures (IV and V) showed two main peaks, their maximum temperatures being located at about 550 and 880 °C. These were accompanied by total weight loss of 46% corresponding to the reduction of $MnO_2$ to $Mn_2O_3$ and formation of $Al_2O_3$ beside $Fe_2O_3$ at about 550 °C. The last thermal decomposition step starts at about 870 °C and followed by weight loss of 1.0%, which might represent the formation of $Mn_3O_4$, $MnAl_2O_4$, and $Fe_3O_4$. These phases will be confirmed later by XRD investigation.

On the other hand, the DTG curves of the mixtures Mn–Fe–Al (IX and X) did not detect the peaks located at 550 and 880 °C. Also, the TG curves of these mixtures did not show noticeable weight loss up to 1000 °C. From the above results, it could be concluded that the presence of iron enhanced the thermal decomposition of aluminum hydroxide to aluminum oxide and manganese nitrate to manganese trioxide and stabilized the latter phase up to high temperature. So, the probability of the formation of manganese ferrite is possible which will be confirmed later by the XRD investigation of the mixtures (IX and X) precalcined at 1000 °C. These results reflect the effect of sequence in the preparation process on the thermal decomposition course.

### 3.6. XRD characterization mixtures of Mn–Al (I) and Fe–Al (IV) influenced by doping with ferric and manganese oxides and preheated at 400–800 °C

Fig. 4a–d shows the X-ray diffractograms of the mixtures Fe–Mn–Al (IV and V) and Mn–Fe–Al (IX and X) thermally treated at 400, 600, and 800 °C. From Fig. 4, it can be seen that the treatment of all mixtures at 400 °C showed the formation of poorly crystalline $\gamma$-$Al_2O_3$ phases. The intensity of the X-ray pattern of this phase was found to be affected by the sequence of the metal oxides supported on alumina. It can be noticed that the degree of crystallinity of the formed phase decreased with increasing the amount of ferric oxide added to the pure mixture Mn–Al (I) and sharp decreasing was observed when manganese oxide doped the mixture Fe–Al (VI). In the same time, well-crystalline $\beta$-$MnO_2$ phase was detected

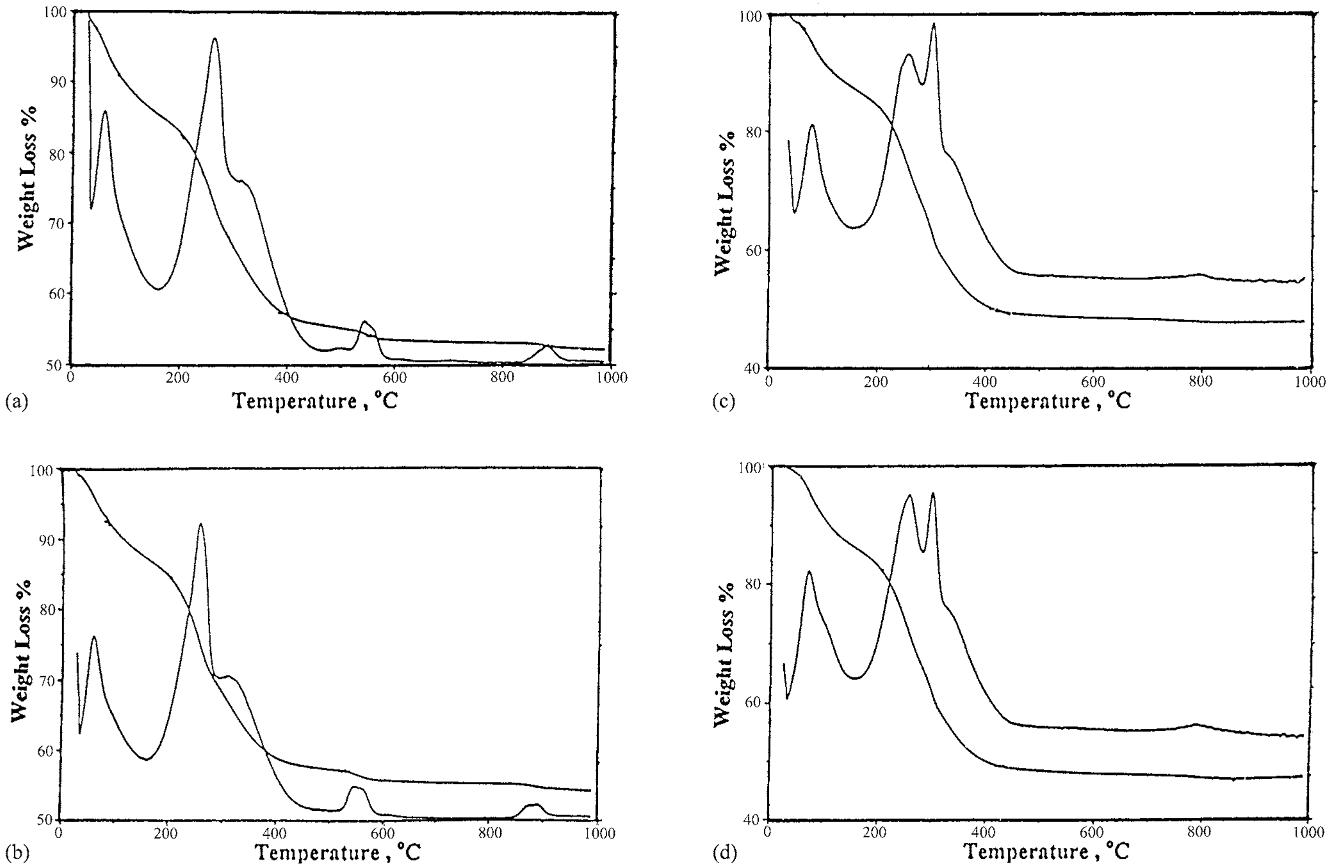

Fig. 3. Thermal analysis (TG–DTG) of mixtures: (a) Fe–Mn–Al (IV); (b) Fe–Mn–Al (V); (c) Mn–Fe–Al (IX); (d) Mn–Fe–Al (X).

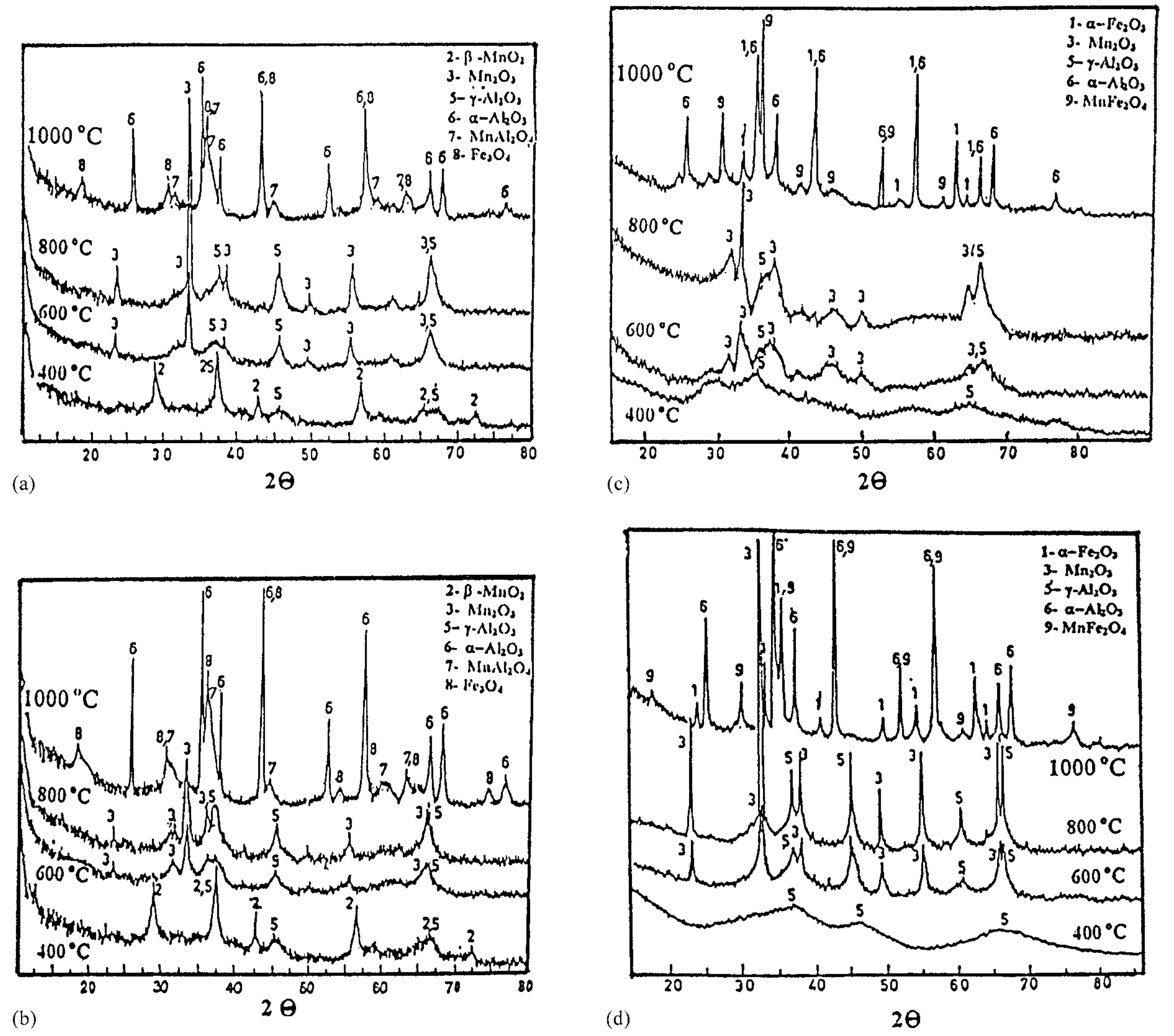

Fig. 4. X-ray diffractograms of mixtures preheated at 400, 600, 800, and 1000 °C: (a) Fe–Mn–Al (IV); (b) Fe–Mn–Al (V); (c) Mn–Fe–Al (IX); (d) Mn–Fe–Al (X).

for all the mixtures preheated at 400 °C, except for the mixtures Mn–Fe–Al (IX and X) precalcined at the same temperature.

The thermal treatment of the above mixtures at 600 and 800 °C led to the formation of only two crystalline $Mn_2O_3$ cubic phase beside $\gamma$-$Al_2O_3$ phases. There are no patterns detected for the ferric oxide as separate phase for all the mixtures thermally treated at 400 °C up to 800 °C. This behavior is in contrast to that of pure ferric nitrate preheated at the same temperature. This behavior reflects the role [17] of $Al_2O_3$ in increasing the degree of dispersion of $Fe_2O_3$ crystallites; in other words, $Al_2O_3$ much decreased the particle size of $Fe_2O_3$ phase to an extent preventing its detection in the XRD investigation. On the other hand, the intensity of $Mn_2O_3$ patterns was found to decrease with increasing the ferric oxide content in the mixture. Also, it can be seen that the degree of crystallinity of the observed phases increased with increasing the calcination temperature up to 1000 °C.

### *3.7. XRD characterization of mixtures of Mn–Al (I) and Fe–Al (IV) influenced by doping with ferric and manganese oxides and preheated at 1000 °C*

From Fig. 4a–d, it can be seen that the mixtures Fe–Mn–Al (IV and V) doped with ferric oxide and preheated at 1000 °C showed the formation of well-crystalline $\alpha$-$Al_2O_3$, $MnAl_2O_4$, and $Fe_3O_4$ phases. On the other hand, X-ray of the mixtures Mn–Fe–Al (XI and X) doped with manganese oxide and thermally treated at the same temperature showed the formation of well-crystalline $\alpha$-$Al_2O_3$, $\alpha$-$Fe_2O_3$, and $MnFe_2O_4$ phases. The above results reflect the role of both of manganese and ferric oxides to enhance the crystallization process of alumina in the alpha-form (corundum) at temperature lower than its formation (>1200 °C) [17,18]. Comparing the obtained results of XRD of the mixture Mn–Al (I) and that doped with ferric oxide, mixtures (IV and V), preheated at 1000 °C. It can be seen that the crystalline $Mn_3O_4$ phase was detected only for the mixture Mn–Al (I). This behavior reflects the role of ferric oxide to stabilize the manganese trioxide, which might be undergo solid–solid interaction with alumina forming manganese aluminate, as previously mentioned. The degree of intensity of manganese aluminate phase increased with increasing the ferric oxide content in the mixture. The absence of manganese ferrite phase in the case of mixtures (IV and V) is quite expected due to the absence of any free manganese oxide and also the formation of crystalline $Fe_3O_4$ phase at this temperature (1000 °C). It seems that the crystallization of $Fe_2O_3$ into $Fe_3O_4$ might suggest that the formation of manganese aluminate enhanced the phase transformation process as follows:

$$3Fe_2O_3 \underset{(MnAl_2O_4)}{\overset{1000^\circ C}{\rightarrow}} 2Fe_3O_4 + \tfrac{1}{2}O_2$$

So, it can be seen that both of manganese aluminate and $Fe_3O_4$ have mutual effect on the formation of each other, at the same time, their formation is quite correlated with the absence of manganese ferrite for the mixtures (IV and V) preheated at 1000 °C. On the other hand, the X-ray diffractogram of the mixtures (IX and X) precalcined at 1000 °C showed the absence of crystalline $Mn_3O_4$, $MnAl_2O_4$, and $Fe_3O_4$ phases. In this case, iron was added before manganese to alumina, so the formed ferric oxide covered the surface of alumina and acted as energy barrier for manganese oxide to interact with $Al_2O_3$ and then the disappearance of $MnAl_2O_4$ phase, which affect the formation of $Fe_3O_4$ as maintained previously, and then a portion of the produced small-sized $Fe_2O_3$ crystallites undergo solid–solid interaction with the manganese oxide forming crystalline manganese ferrite phase according to the following equation [12]:

$$Mn_2O_3 + 2Fe_2O_3 \overset{1000^\circ C}{\rightarrow} 2MnFe_2O_4 + O_2$$

### *3.8. Catalytic activities measurements*

Table 2 shows that the rate constant $k$ (min$^{-1}$) of hydrogen peroxide decomposition reaction over pure oxides obtained by calcination of their salts at 400–880 °C, which are lower than that of mixed and doped oxides supported on alumina. In most cases, it could be seen that the catalytic activity increased with increasing the reaction temperature from 30 up to 50 °C.

#### *3.8.1. Catalytic activity over single oxides*

The experimental results of the catalytic decomposition of $H_2O_2$ over hydrated ferric nitrate and aluminum hydroxide preheated at 400–1000 °C did not show noticeable catalytic activity because of formation of inactive species of $Fe_2O_3$ and $Al_2O_3$ [12,17]. On the other hand, pure manganese nitrate preheated at 400 and 600 °C showed high catalytic activity, which attributed to the formation of $MnO_2$ and $Mn_2O_3$, respectively. Further increase of treatment temperature up to 1000 °C leads to a sharp decrease in activity because of the increasing of degree of crystallinity of active species, formation of $Mn_3O_4$ and/or sintering process [10,19].

#### *3.8.2. Catalytic activity of pure Mn-oxide/$Al_2O_3$ and $Fe_2O_3$/$Al_2O_3$ systems*

Table 2 showed that the rate of hydrogen peroxide decomposition reaction over Mn-oxide/$Al_2O_3$ system obtained at different temperatures increased with increasing the treatment up to 800 °C and also increased with increasing the reaction temperatures from 30 up to 50 °C. The X-ray results of this solid preheated at 400 and 600 °C possess phases of $MnO_2$ and $Mn_2O_3$, which are very active in this reaction. In this case, according to Kanungo et al. [20], the decomposition may take place by donating an electron from

Table 2
The dependence of rate constant (*k*) on the catalyst composition, calcination temperatures, and reaction temperatures

| Catalyst from | Calcination temperature (°C) | $k \times 10$ (min$^{-1}$) | | | ln *A* | *E* (kJ mol$^{-1}$) |
|---|---|---|---|---|---|---|
| | | 30 °C | 40 °C | 50 °C | | |
| $Mn(NO)_3 \cdot 4H_2O$ | 400 | 1.5 | 1.7 | 2.2 | 6 | 20 |
| | 600 | 1.0 | 1.5 | 1.9 | 9 | 28 |
| | 800 | 0.6 | 1.1 | 1.5 | 13 | 40 |
| Mn–Al (I) | 400 | 2.6 | 3.3 | 4.7 | 8 | 24 |
| | 600 | 3.2 | 5.0 | 7.9 | 14 | 37 |
| | 800 | 4.0 | 6.2 | 9.9 | 15 | 40 |
| 0.025 Fe–Mn–Al (II) | 400 | 3.4 | 5.2 | 8.4 | 14 | 37 |
| | 600 | 4.1 | 7.5 | 10.8 | 15 | 40 |
| | 800 | 5.1 | 9.0 | 14.0 | 21 | 54 |
| 0.05 Fe–Mn–Al (III) | 400 | 2.1 | 3.0 | 4.3 | 10 | 29 |
| | 600 | 2.7 | 4.4 | 6.3 | 13 | 35 |
| | 800 | 4.1 | 5.4 | 8.5 | 11 | 31 |
| 0.10 Fe–Mn–Al (IV) | 400 | 1.5 | 2.4 | 3.4 | 11 | 33 |
| | 600 | 1.3 | 1.8 | 2.3 | 8 | 25 |
| | 800 | 0.8 | 1.2 | 1.7 | 11 | 34 |
| 0.25 Fe–Mn–Al (V) | 400 | 0.9 | 1.3 | 1.8 | 10 | 32 |
| | 600 | 0.4 | 0.7 | 1.1 | 13 | 42 |
| | 800 | 0.2 | 0.4 | 0.7 | 16 | 50 |
| Fe–Al (VI) | 400 | 0.3 | 0.4 | 0.5 | 8 | 31 |
| | 600 | 0.1 | 0.2 | 0.20 | 8 | 33 |
| | 800 | 0.06 | 0.1 | 0.14 | 9 | 35 |
| 0.025 Mn–Fe–Al (VII) | 400 | 0.8 | 1.3 | 1.8 | 12 | 36 |
| | 600 | 0.4 | 0.6 | 0.9 | 12 | 38 |
| | 800 | 0.2 | 0.4 | 0.7 | 16 | 50 |
| 0.05 Mn–Fe–Al (VIII) | 400 | 1.0 | 1.7 | 3.2 | 17 | 49 |
| | 600 | 0.6 | 1.1 | 1.8 | 15 | 46 |
| | 800 | 0.33 | 0.6 | 1.0 | 13 | 46 |
| 0.10 Mn–Fe–Al (IX) | 400 | 1.39 | 1.9 | 2.60 | 8 | 26 |
| | 600 | 0.86 | 1.4 | 2.05 | 12 | 36 |
| | 800 | 0.44 | 1.0 | 1.48 | 17 | 50 |
| 0.25 Mn–Fe–Al (X) | 400 | 2.20 | 3.0 | 4.00 | 9 | 25 |
| | 600 | 1.43 | 2.0 | 3.10 | 11 | 33 |
| | 800 | 0.60 | 1.0 | 1.12 | 8 | 26 |
| $Fe(NO_3)_3 \cdot 9H_2O$ | 400 | 0.06 | 0.2 | 0.20 | 15 | 50 |
| | 600 | 0.03 | 0.1 | 0.16 | 22 | 69 |
| | 800 | 0.01 | 0.04 | 0.07 | 26 | 80 |

the substrate to the solution or vice versa. Then, if the catalyst accepts an electron, the possible active site is $Mn^{4+}$ to yield a $HO_2$ radical according to the following equation:

$$Mn^{4+} + H_2O_2 \rightarrow H^+ + HO_2^{\bullet} + Mn^{3+}$$

The observed increase in the activity of $Mn_2O_3/Al_2O_3$ system due to heating at 800 °C might be attributed to a possible formation of metal oxide–support compound. This system possesses activity higher than that of the pure oxides obtained at the same calcination temperatures. Because, these conditions favor the increase of the active site concentration of manganese trivalent which yields an OH radical as follows:

$$\mathrm{Mn}^{3+} + \mathrm{H_2O_2} \rightarrow {}^{\bullet}\mathrm{OH} + {}^{-}\mathrm{OH} + \mathrm{Mn}^{4+}$$

On the other hand, it can be observed from Table 2 that the rate of $H_2O_2$ decomposition over $Fe_2O_3/Al_2O_3$ system obtained at different treatment temperatures was found to be much lower than that of $Mn_2O_3/Al_2O_3$. However, the activity of this system is higher than that of pure ferric nitrate preheated at the same temperature. This is explained in term that alumina greatly increases the degree of dispersion of active constituents, hindering their grain growth and thus increasing the activity of the supported system by increasing the concentration of catalytically active constituents of $Mn^{3+}$–$Mn^{2+}$ or $Fe^{3+}$–$Fe^{2+}$ ion pairs [18,21].

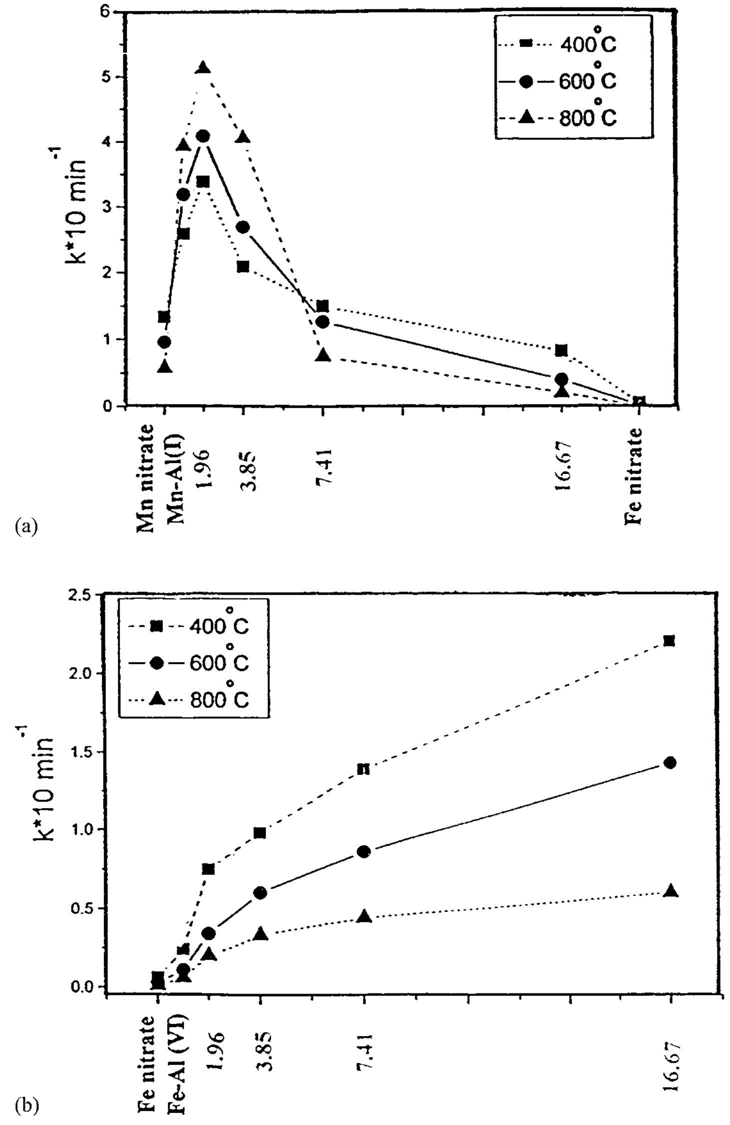

Fig. 5. (a) Effect of ferric oxide doping on the catalytic activity of Mn-oxide/$Al_2O_3$ obtained at 400, 600, and 800 °C; (b) effect of manganese oxide doping on the catalytic activity of $Fe_2O_3/Al_2O_3$ obtained at 400, 600, and 800 °C.

### 3.8.3. *Effect of $Fe_2O_3$ doping on the activity of Mn-oxide/$Al_2O_3$ systems*

The effect of $Fe_2O_3$ doping on Mn-oxide/$Al_2O_3$ system obtained at reaction temperatures 400–800 °C has been represented in Fig. 5a, which shows that the catalytic activity of Mn-oxide/$Al_2O_3$ system obtained at different calcination temperatures (400–800 °C) increases progressively by increasing the amount of dopant present reaching to a maximum limit at 1.96 mol%, then significantly decreases with increase in the dopant concentration above this limit. The observed increase in the activity can express the induced increase with concentration of catalytically active constituents taking part in the catalysis of $H_2O_2$ decomposition reaction. This assumption is evidenced from the fact that $\Delta E$ (clustered in Table 2) is dependent on the $A$ term of the exponential factor in Arrhenius equation. The created active sites due to ferric oxide doping could be $Fe^{3+}$–$Mn^{3+}$, $Fe^{3+}$–$Mn^{2+}$, $Fe^{3+}$–$Fe^{2+}$, $Mn^{3+}$–$Mn^{2+}$ ion pairs. However, the observed significant decrease in the catalytic activity on increasing the ferric oxide dopant from 3.85 to 16.67 mol% might be attributed to decrease in the concentration of highly active species of manganese due to the process of blocking of the active constituents by the high concentration of small active dopants.

### 3.8.4. *Effect of Mn-oxide doping on the activity of $Fe_2O_3$/$Al_2O_3$ systems*

In contrast to the above case, Fig. 5b shows that the loading of the manganese oxide on $Fe_2O_3$/$Al_2O_3$ system obtained at 400–800 °C significantly increased the catalytic activity of the system on increasing the concentration of dopant from 1.96 to 16.67 mol% at different treatment temperatures. This might be attributed to the role of manganese species previously mentioned. In this case, the concentration of active species, specially of manganese sites, progressively increased leading to increasing the activity. From Table 2, it can be seen that $\Delta E$ values increased on increasing the amount of manganese oxide species.

Finally, it was found that the catalytic activity of all the samples thermally treated at 1000 °C sharply decreased. This might be attributed to the formation of inactive species, such as $MnAl_2O_4$, $MnFe_2O_4$ and/or sintering process [10,15].

## 4. Conclusion

1. Ferric oxide doping enhanced the thermal decomposition of aluminum hydroxide to aluminum oxide and enhanced the crystallization of aluminum oxide in the alpha-form at temperature lower than its formation.
2. Ferric oxide doping enhanced the catalytic activity of Mn-oxide/$Al_2O_3$ system obtained at 400–800 °C up to certain limit of dopant. Then, it progressively decreased on further increase of the dopant concentration.
3. Crystallines manganese aluminate and manganese ferrite phases were formed as a result of thermal solid–solid interactions between the corresponding oxides at 1000 °C. These phases affected the phase transformation of $Fe_2O_3$ to $Fe_3O_4$ in the mixed solids precalcined at 1000 °C.
4. Aluminum hydroxide retarded the thermal decomposition of ferric nitrate to ferric oxide and also retarded that of manganese nitrate to manganese dioxide.
5. Manganese oxide enhanced the ordering of $Al_2O_3$ in alpha-form at 1000 °C. Manganese oxide-doped $Fe_2O_3$/$Al_2O_3$ system obtained at 400–800 °C with manganese oxide enhanced the catalytic activity of the system.

## References

[1] G.A. El-Shobaky, A.N. Al-Noomi, Appl. Catal. 29 (1987) 235.
[2] G.A. El-Shobaky, G.A. Fagel, Thermochim. Acta 141 (1989) 205–216.
[3] N.A. Youssef, M.M. Selim, S.M. Sayed, Bull. NRC (Egypt) 16 (12) (1991) 131–142.
[4] X. Youchang, Q. Minxie, T. Yougi, Sci. Sin. 27 (1984) 549.
[5] H.G. El-Shobaky, M. Mokhtar, S. Ahmed, Thermochim. Acta 327 (1999) 39–46.
[6] M.I. Zaki, A.K.H. Nohman, G.A.M. Hussein, Y.E. Nashed, J. Mater. Sci. Lett. 14 (17) (1995) 118–192.
[7] J. Laine, F. Severino, A. Lopez-Agudo, J.L.G. Fierro, J. Catal. 129 (1) (1991) 297–299.
[8] L. Lycourghiotis, V. Dimitris, A. Nicholas, Z. Phys. Chem. 125 (1998) 95.
[9] G.A. El-Shobaky, A.N. Noaimi, Surf. Technol. 26 (3) (1985) 235.
[10] W.M. Shaheen, M.M. Selim, Thermochim. Acta 322 (1998) 117–128.
[11] K. Nobuyoshi, O. Shougo, N. Tatsuya, T. Haruhiko, Thermochim. Acta 267 (1995) 195–208.

[12] M.M. Selim, L.B. Khalil, AFINIDAD 40 (433) (1991) 167–172.
[13] W.M. shaheen, M.M. Selim, J. Therm. Anal. Colorimetry 29 (2000) 961–970.
[14] M.M. Selim, M.K. El-Aiashy, Mater. Lett. 21 (1995) 262–270.
[15] M.M. Selim, N.A. Hassan, W. Mokhtar, A.A. Attia, Bull. NRC (Egypt) 21 (1996) 1.
[16] G.A. El-Shobaky, Th. El-Nabaraway, N. Goneim, I.M. Morsi, Surf. Technol. 19 (1983) 109.
[17] W.M. Shaheen, M.M. Selim, AFINIDAD 54 (479) (1999) 39–44.
[18] G.A. El-Shobaky, G.A. Fagal, N. Petro, A.M. Dessouki, Radiat. Phys. Chem. 29 (1987) 39.
[19] V. Mucka, K. Lang, Collect. Chem. Commun. 33 (8) (1988) 1836–1846.
[20] S.B. Kanungo, K.M. Parida, B.R. Sant, Electrochim. Acta 26 (8) (1981) 1157.
[21] V. Mucka, Collect. Chem. Commun. 51 (1986) 1874–1882.